

Toxicology Research

Accepted Manuscript



This is an *Accepted Manuscript*, which has been through the Royal Society of Chemistry peer review process and has been accepted for publication.

Accepted Manuscripts are published online shortly after acceptance, before technical editing, formatting and proof reading. Using this free service, authors can make their results available to the community, in citable form, before we publish the edited article. We will replace this *Accepted Manuscript* with the edited and formatted *Advance Article* as soon as it is available.

You can find more information about *Accepted Manuscripts* in the [Information for Authors](#).

Please note that technical editing may introduce minor changes to the text and/or graphics, which may alter content. The journal's standard [Terms & Conditions](#) and the [Ethical guidelines](#) still apply. In no event shall the Royal Society of Chemistry be held responsible for any errors or omissions in this *Accepted Manuscript* or any consequences arising from the use of any information it contains.

Endosulfan induced the arrest of cell cycle through inhibiting the signal pathway mediated by PKC- α and damaging the cytoskeleton in spermatagonial cell of mice *in vitro*

Fang-Zi Guo^{a, b}, Lian-Shuang Zhang^{a, b}, Jia-Liu Wei^{a, b}, Yan-Bo Li^{a, b}, Zhi-Xiong Shi^{a, b}, Yu-Mei Yang^{a, b}, Xian-Qing Zhou^{a, b, *}, Zhi-Wei Sun^{a, b}

^a Department of Toxicology and Hygienic Chemistry, School of Public Health, Capital Medical University, Beijing, China. 100069

^b Beijing Key Laboratory of Environmental Toxicology, Capital Medical University, Beijing 100069, China

* Corresponding author: Xian-Qing Zhou, Department of Health Toxicology and Health Chemistry, School of Public Health, Capital Medical University, No.10 Xitoutiao, You'anmen Wai, Fengtai District, Beijing 100069, PR China.

Abstract

The previous studies have showed that endosulfan has adverse effects on male reproductive system and the oxidative stress induced by endosulfan is related to its toxicity. However, the molecular mechanism of endosulfan reproductive toxicity is still unknown. To investigate its mechanism of toxicity, the GC-1spg cells were exposed to 0, 6, 12 and 24 μ g/mL endosulfan for 24h, respectively. Results showed that endosulfan resulted in a dose-dependent reduction in cell viability and increases

in LDH release, apoptosis rate, the malondialdehyde (MDA) level, the reactive oxygen species(ROS) production and DNA damage degree including the percentage of tail DNA, tail length, tail moment (TM) and Olive tail moment (OTM). Endosulfan induced the arrests of both S and G2/M phase and proliferation inhibition. The expression of PKC- α , CDK2, Cyclin E, RAF-1, MEK1/2, *p*-MEK1/2, ERK1/2 and *p*-ERK1/2 in GC-1spg cells declined remarkably after treatment with endosulfan. Endosulfan also damaged the microfilament, microtubule and cell nucleus, and blocked the mitosis process. The results suggested that endosulfan could induce the cell cycle arrest and proliferation inhibition by inhibiting the protein expression of cellular signaling pathway mediated by PKC- α because of DNA damage resulted from oxidative stress; meanwhile, endosulfan could also lead to mitotic arrest through directly damaging the cytoskeleton and cell nucleus resulted from oxidative stress; which therefore induced cytotoxicity of GC-1spg cells.

Key Words: Spermatagonial cells, cytotoxicity, cell cycle arrest, cytoskeleton, cellular signaling pathway

Introduction:

Endosulfan(6,7,8,9,10,10-hexachloro-1,5,5a,6,9,9a-hexahydro-6,9-methano-2,4,3-benzodioxathiepin-3-oxide,C₉H₆Cl₆O₃S), which is an organochlorine insecticide, is still extensively used in some developing countries despite it is defined as a persistent organic pollutant (POP) by the Stockholm Convention on POPs in April 2011.^{1,2}

Contamination of the air, water and soil environments by endosulfan occurs generally as a result of runoff from the agricultural fields and/or discharge during its manufacture.³ Endosulfan exists in water with a half-life of more than 14 d and persists longer in soil with a half-life of approximately 60–800 d.⁴ Because endosulfan is highly lipophilic, it bioaccumulates and biomagnifies along the alimentary chain.⁵ It has been detected in different matrices (water bodies: 1.7, soil: 0.3–34.9, fruits: 0.36–212.3, milk: 0.4–56.2, butter: 0.6–13.4; Laddu: 676.0, human blood in Kasargod district of Kerala, India: 0.69–176.2 $\mu\text{g/mL}$).^{6,7} The data obtained from the global monitoring network programme for POPs also showed that endosulfan was still abundant in the environment and that it was used a lot in some countries.⁸

Endosulfan has been implicated in genotoxicity,⁹ neurotoxicity,¹⁰ hepatotoxicity,¹¹ immunotoxicity,¹² reproductive toxicity¹³ and teratogenicity^{14, 15} on exposed organisms. With the increasingly serious environmental pollution and reduction of biodiversity, there is growing concern that chemicals, whether natural or human-made, may be causing damage to reproductive system of wildlife and human. Moreover, the male reproductive system has raised major concerns from both the research community and the public.¹⁶ The previous studies showed that endosulfan caused reductions in the motility, viability and daily sperm production (DSP), damaged the integrity of sperm chromatin, decreased the level of serum testosterone and testicular weight, inhibited the spermatogenesis and increased sperm abnormalities.^{17, 18}

Moreover, accumulating evidence suggested that oxidative stress induced by

endosulfan was related to its toxicity¹⁹ and endosulfan could indirectly cause a decline in reproductive function by damaging the structure of mitochondria, resulting in energy metabolism dysfunction.²⁰ Study also reported that endosulfan upregulates AP-1 binding and ARE-mediated transcription via ERK1/2 and p38 activation in HepG2 cells.¹⁵ However, the molecular signaling pathways of endosulfan-induced reproductive toxicity on spermatogonial cells have maintained unknown. Besides, the data which associate cell-cycle signaling pathways with endosulfan have not been reported so far. Therefore, the present experiment was designed to research the effects of endosulfan on the cell cycle and related cellular signaling pathways mediated by PKC- α in spermatogonial cell *in vitro*, so as to explain the toxic mechanism of endosulfan.

Materials and Methods

Cell Culture and Treatment

The spermatogonial cell GC-1spg line was purchased from American Type Culture Collection (ATCC® Number: CRL-2196™). The cells were maintained in Dulbecco's Modified Eagle's Medium (DMEM) (Gibco, USA) supplemented with 10% fetal bovine serum (Gibco, USA), 100 U/mL penicillin and 100 μ g/mL streptomycin, and cultured at 37°C in 5% CO₂ humidified environment. For experiments, the cells were seeded in 6-well plates (except MTT assay using 96-well plates) at a density of 1×10^5 cells/mL and allowed to attach for 24 h, then treated with various concentrations of endosulfan (3, 6, 12, 24, 36, 48, 60 and 72 μ g/mL) for

another 24 h, respectively. Endosulfan (analytical standard, purity: 96%) was obtained from Jiangsu Kuaida Agrochemical Co., Ltd. (Nantong, China), and dissolved in DMSO and diluted with DMEM. Vehicle controls were supplied with an equivalent volume of DMEM which included 0.24 % DMSO. Each group had five replicate wells. All experiments were repeated at least three times.

Determination of Cell Viability

The cell viability was determined using 3-(4,5-Dimethylthiazol-2-yl)-2,5-diphenyltetrazolium bromide, a yellow tetrazole (MTT) assay performed as previously described.²¹ The absorbance of formazan was measured at 492 nm by a microplate reader (Thermo Multiskan MK3, USA).

Determination of LDH Release

The integrity of the cell membrane, which is identified by the measurement of lactate dehydrogenase (LDH) activity in the extracellular medium, was measured using LDH Kit (Jiancheng, China) according to the manufacturer's protocols. After exposure to different concentrations of endosulfan for 24 h, 100 μ l of cell culture media was used to analyze LDH activity, and the absorbance at 440 nm was determined using a UV-visible spectrophotometer (Beckman DU-640B, USA).

Determination of Cell Apoptosis

Apoptosis in GC-1spg cells was determined using the Annexin V-propidium iodide (PI) apoptosis detection kit (KeyGen, China). After centrifugation at 1000 rpm for 5 min, the cells were washed twice with PBS and suspended with 500 μ L binding buffer, then incubated with 5 μ L Annexin V-FITC and 5 μ L PI for 15 min in the dark at room

temperature and analyzed using a flow cytometer (Millipore, USA), and at least 1×10^4 cells were counted for each sample. The different cell populations were identified by the different labeling patterns in the Annexin V-PI analysis. For example, FITC negative and PI negative were designated as live cells in the lower left quadrant; FITC positive and PI negative as early apoptotic cells in the lower right quadrant; FITC positive and PI positive as late apoptotic cells in the upper right quadrant; and FITC negative and PI positive as cells fragments in the upper left quadrant. The sum of early apoptosis rate and late apoptosis rate was finally calculated as the total rate of apoptosis.

Determination of Oxidative Damage

The malondialdehyde (MDA) (an end product of lipid peroxidation) content was determined using commercially available kits (Jiancheng, China) according to the manufacturer's instructions. After exposure to endosulfan for 24 h, the cells were washed once with ice-cold PBS, and lysed in ice-cold RIPA lysis buffer which contained 1 mM phenylmethylsulphonyl fluoride (PMSF) (Dingguo changsheng biotech CO.LTD, China) for 30 min. After centrifugation at 12,000 rpm, 4°C for 10 min, the supernatants were collected to measure the MDA content.

The oxidative stress is related to overproduction of reactive oxygen species (ROS). The generation of intracellular ROS was measured through fluorescence intensity of dichlorofluorescein (DCF) by flow cytometry using the 2, 7-dichlorofluorescein diacetate (DCFH-DA) (Beyotime, China). After exposure to endosulfan for 24 h, the

cells were incubated with medium which contained DCFH-DA at a concentration of 5 μM for 40 minutes at 37 °C in the dark. Then the cells were washed twice with cold PBS and resuspended in the PBS for further analysis. At last, fluorescent intensity of at least 1×10^4 cells for each sample were measured by flow cytometry (Becton-Dickison, USA).

Determination of DNA Damage

Comet assay, also known as single cell gel electrophoresis (SCGE), is a sensitive technique for determining DNA breakage in individual cells. The DNA damage induced by endosulfan was measured by Single cell gel electrophoresis kit (Biolab, China). After GC-1spg cells were collected, they were resuspended in PBS, 20 μL of the cells suspension and 80 μL of low melting agarose were mixed, and 80 μL of the suspension was pipetted onto a comet-slide. Then the slides were placed in dark at 4 °C for 10 min, and then placed in pre-chilled lysing solution at 4 °C for 2h. The slides were removed from lysing solution, tapped on a paper towel and immersed in alkaline solution for 45 min in dark at room temperature. After washed twice for 5 min per time, the slides were electrophoresed at low voltage (300 mA, 25 V) for 30 min. Then the slides were removed from the electrophoresis unit and tapped at room temperature. Subsequently, the air-dried slides were stained with propidium iodide (PI) and assessed by a fluorescence microscope (Olympus IX81, Japan). To prevent additional DNA damage, all the steps were performed under dimmed light. The data were analyzed using CASP software based on 100 randomly selected cells per sample. The percentage of tail DNA, tail length, tail moment (TM) and Olive tail moment (OTM)

were selected as indicators of DNA damage.

Determination of Cell Cycle

The cell-cycle distributions were measured by the cell cycle detection kit (KeyGen, China). After centrifugation at 1000 rpm for 5 min, the cells were washed once with PBS and fixed in 70% ethanol (placed in -20°C for 24h in advance) for 24 h. Then the cells were washed twice with PBS and treated with 100µL of RNase A at 37°C for 30 min. Finally, the cells were stained with 400µl of propidium iodide (PI) and incubated in dark for 30 min. At least 1×10^4 cells for each sample were analyzed by flow cytometry (Beckman Coulter, USA).

Assessment of Microfilament, Microtubule and the Cell Nucleus Damage

After washed twice with PBS and fixed with 3.7% formaldehyde solution at room temperature for 10 minutes, the cells were washed twice again with PBS(containing 0.1% TritonX-100) for 5 minutes per time, and stained with 5 µg/mL Hoechst 33258 solution (Beyotime, China) for 20 minutes. Then the cells were washed twice with PBS (containing 0.1% TritonX-100) for 5 minutes per time and stained with 200 nM of Actin-Tracker Green (Enogene Biotech. Co.,Ltd, China) in the dark for 30 minutes at 37 °C. Subsequently, the cells were washed twice with PBS (containing 0.1% TritonX-100) for 5 minutes per time and stained with 250 nM of Tubulin-Tracker Red (Enogene Biotech. Co.,Ltd, China) in the dark for 30 minutes at 37 °C. Finally, the cells were visualized using a laser confocal microscope (Leica, Germany) and selected randomly for further observation.

Assessment of Mitosis Process

After exposed to 24 $\mu\text{g}/\text{mL}$ endosulfan, the GC-1spg cells were observed using a real-time inverted phase contrast microscope (UltraVIEW VoX, USA) for 24h to determine whether there were abnormal mitosis phenomenon. Six visual fields were selected randomly and took pictures every 10 minutes.

Determination of Cell Proliferation

After centrifugation at 1200 rpm for 5 min, the GC-1spg cells were marked with 5 μM of CFDASE probe diluent (KeyGen, China) at 37 $^{\circ}\text{C}$ for 15 min. Then the cells were washed twice with PBS, seeded in 6-well plates at a density of 1×10^5 cells/mL and allowed to attach for 24 h. After the cells were treated with endosulfan for 24 h and centrifuged at 1200 rpm for 5 min, 500 μL of PBS were added in to suspend the cells. Finally, the average fluorescence intensity of cells per sample was detected by flow cytometry (BDFACSAria, USA).

Determination of Protein Expression in Cellular Signaling Pathway

The protein levels of PKC- α , Cyclin E, CDK2, RAF-1, ERK1/2, *p*-ERK1/2, MEK1/2, and *p*-MEK1/2 in GC-1spg cells were determined by western blot analysis. Total protein of GC-1spg cells was extracted using a Protein Extraction Kit (KeyGen, China) and measured by the bicinchoninic acid (BCA) protein assay (Dingguo changsheng biotech CO.LTD, China). The equal amounts of lysate proteins (20 μg) were loaded onto SDS-polyacrylamide gels (12% separation gels) and electrophoretically transferred to polyvinylidene fluoride (PVDF) membranes (Millipore, USA). After blocked with 5% nonfat milk in TBST(Tris-buffered saline containing 0.05% Tween-20) for 1 h at room temperature, the membrane was

incubated with β -actin[1:1000, rabbit antibodies, Cell Signaling Technology (CST), USA], PKC- α (1:2000, rabbit antibodies, Abcam, USA) , Cyclin E[1:1000, rabbit antibodies, Cell Signaling Technology (CST), USA], CDK2 (1:500, rabbit antibodies, Abcam, USA) , RAF-1[1:500, rabbit antibodies, Santa Cruz Biotechnology(SCBT), USA], ERK1/2[1:1000, rabbit antibodies, Cell Signaling Technology (CST), USA], *p*-ERK1/2[1:1000, rabbit antibodies, Cell Signaling Technology (CST), USA], MEK1/2 (1:1000, rabbit antibodies, Abcam, USA) and *p*-MEK1/2 (1:1000, rabbit antibodies, Abcam, USA) overnight at 4°C, respectively, washed three times with TBST for 10min per time, and incubated with a horseradish peroxidase-conjugated anti-rabbit IgG secondary antibody [1:5000, Immunology Consultants Laboratory(ICL), USA]for 1h at room temperature. After washed three times with TBST for 10 min per time, the antibody-bound proteins were detected with the ECL chemiluminescence reagent (Pierce, USA).

Statistical Analysis

All data were analyzed using SPSS (Statistical Package for the Social Sciences software, version 17.0 for Windows). One-way analysis of variance (ANOVA) was used to test the significant difference among all groups, followed by least significant difference (LSD) test to detect significant difference between two groups. All values were expressed as mean \pm standard error (S.E.), and the results were considered significant at $P < 0.05$. Based on the MTT results, the values from LC10 to LC90 were calculated by probit analysis using SPSS software, and the confidence intervals were 95% according to the method used by Nath and Kannan.^{22, 23}

Results

Cytotoxicity

Cell viability gradually decreased with the increase of endosulfan level in a dose-dependent manner compared with the control group, and in endosulfan treated groups ($>3\mu\text{g/mL}$) were remarkably lower than that of control group and significantly different from each other (Figure 1A). In addition, the LC50 was $32.829\mu\text{g/mL}$ (Table 1). Based on the MTT results, endosulfan concentrations were chosen at 6, 12 and $24\mu\text{g/mL}$ for the next experiments. Moreover, the MTT result was in accordance with the increased cytomembrane damage measured by LDH activity. The LDH activity increased apparently in 12 and $24\mu\text{g/mL}$ endosulfan treated group compared to control group (Figure 1B). The total apoptotic rates in GC-1spg cells increased with the increase of endosulfan level (Figure 4A), and significantly enhanced in 12 and $24\mu\text{g/mL}$ endosulfan treated group when compared to control group (Figure 1C). The total apoptosis levels of GC-1spg cells were 1.82%, 5.25%, 8.04% and 28.71%, respectively, after exposure to 0, 6, 12 and $24\mu\text{g/mL}$ endosulfan.

Oxidative Stress and DNA Damage

Oxidative damage was evaluated by measuring the intracellular MDA level and the generation of ROS. The MDA level gradually increased with the elevation of endosulfan level, and significantly enhanced in 12 and $24\mu\text{g/mL}$ endosulfan treated group when compared to control group (Figure 1D). The intracellular ROS levels of all endosulfan-treated groups were remarkably increased in a dose dependent manner

when compared to control group. In 24 μ g/mL treated group, the fluorescence intensity was about 3-fold much higher than that of control (Figure 1E). The degree of DNA damage involving the length of tail, the percentage of tail DNA, tail moment (TM) and Olive tail moment (OTM) had no significant difference in 6 and 12 μ g/mL endosulfan treated group compared with the control group. While in 24 μ g/mL endosulfan treated group, the degree of DNA damage significantly elevated (Table 2).

Cell Cycle Arrest and Proliferation Inhibition

Results showed that the percentage of GC-1spg cells in G₀/G₁ phase declined in a dose-dependent manner, whereas the percentages of GC-1spg cells in S and G₂/M phase increased when compared with the control group (Figure 5C). The percentages of GC-1spg cells had a significant increase in S phase in 24 μ g/mL endosulfan treated group and G₂/M phase in 6, 12, 24 μ g/mL endosulfan treated group when compared to control group (Figure 2B). Results also showed that the average fluorescence intensity of cells in groups exposed to 12 μ g/mL and 24 μ g/mL endosulfan increased significantly in comparison with the control group (Figure 2A), which indicated that cell proliferation in this two groups were significantly inhibited.

Changes of the Microfilament, Microtubule, Nucleus and Mitosis process

Results indicated that compared with the control group, the fluorescence intensity of microfilaments and microtubules weakened gradually in cells after treatment with

various concentrations of endosulfan, which showed that the number of microfilaments and microtubules reduced gradually with the increase of endosulfan concentration. Consistently, the maldistribution phenomena of microfilaments and microtubules were more obvious with the increase of endosulfan concentration, even there were accumulations of microfilaments and microtubules, and extinctions of microfilaments and microtubules (Figure 3A and 3B). Moreover, compared with the control group, the size and morphology of nuclei was obviously different in cells after exposure to endosulfan. The cells in control group had round and homogeneously stained nuclei, whereas the phenomenon of nucleus pycnosis was frequently observed in 12 and 24 $\mu\text{g}/\text{mL}$ endosulfan treated group (Figure 3C).

Results also indicated that, after treatment with 24 $\mu\text{g}/\text{mL}$ endosulfan, some cells failed to complete mitosis process normally and died finally (Figure 3E).

Changes of Protein Expression in Cellular Signaling Pathway Mediated by PKC- α

Results showed that the expression of PKC- α , CDK2, Cyclin E, RAF-1, MEK1/2, *p*-MEK1/2, ERK1/2 and *p*-ERK1/2 in GC-1spg cells declined gradually with the increase of endosulfan concentration (Figure 4A). The expression of CDK2 in GC-1spg cells was obviously inhibited in 6, 12 and 24 $\mu\text{g}/\text{mL}$ endosulfan treated group (Figure 4B). The expression of PKC- α , Cyclin E, RAF-1, MEK1/2, *p*-MEK1/2, ERK1/2 and *p*-ERK1/2 in GC-1spg cells decreased remarkably in 12 and 24 $\mu\text{g}/\text{mL}$

endosulfan treated group(Figure 4B).

Discussions

The purpose of this study was to investigate the molecular mechanism by which endosulfan induced the male reproductive toxicity. Health of spermatogonial cells may affect the quality of gametes. So we studied the molecular mechanism *in vitro* with the GC-1spg cells.

First of all, to demonstrate the potential cytotoxicity of endosulfan on GC-1spg cells, the cell viability, LDH activity and apoptosis rates were measured. Results showed that endosulfan resulted in reduction in cell viability and increases in LDH activity and the apoptotic rates in GC-1spg cells. To further confirm whether the oxidative stress was one of mechanisms by which endosulfan induced male reproductive toxicity, we measured the levels of MDA (a biomarker of oxidative stress) and ROS which mediated oxidative stress.²⁴ The result showed that endosulfan could raise the MDA and ROS level, suggesting that endosulfan induced oxidative stress. Takhsid also showed that endosulfan could increased testis MDA, while supplementation of vitamin C and vitamin E to endosulfan-treated rats could reduce the toxic effect of endosulfan on lipid peroxidation in the testis.¹⁹ Recognizing that the reactive oxygen could directly induce DNA base oxidation, deamination and indirectly lead to base alkylation via lipid peroxidation (LPO),²⁵ we sought to examine whether the DNA was damaged in GC-1spg cells treated with endosulfan. We did find the higher

concentration of endosulfan produced more severe damage on DNA of GC-1spg cells, which was similar to those of Tao, who showed that the DNA damage in both tissues had excellent correlation with endosulfan concentration.²⁶

Studies had shown that, in response to transient or low levels of DNA damage, cells had a reversible cell cycle arrest whereas a sustained cell cycle arrest followed prolonged or high levels of DNA damage.²⁷ For DNA damage was closely related to cell cycle arrest, especially G1 phase, S phase and G2 phase, and cell cycle was regulated by Cell-cycle checkpoints.²⁸ The function of these checkpoints was to test the damaged or abnormally structured DNA, and to control cell-cycle progression with DNA repair.²⁸ To get a closer insight into the toxic mechanisms of endosulfan on GC-1spg cells, cell cycle distribution was measured. We found that endosulfan blocked the GC-1spg cells at both S and G2/M two phases. Several evidences indicated that the main components of cell cycle control machinery were the Cyclins and CDKs, which constituted active kinase complexes during specific phases of the cell cycle.²⁹ Among them, Cyclin E/CDK2, had an indispensable function in the transition from G1 into S phase.¹⁵ Besides, there were protein kinases C (PKC) as key regulators of critical cell cycle phases, including G1/S transition and G2/M progression.³⁰⁻³³ Among them, PKC- α was known for its involvement in G1/S transition.³⁴ So the expression of Cyclin E, CDK2 and PKC- α were measured. Results showed that endosulfan induced down-regulation of Cyclin E, CDK2 and PKC- α expression in GC-1spg cells. The results above suggested that endosulfan blocked the

cell cycle at S phase through the down-regulation of Cyclin E/CDK2 and PKC- α expression, which was similar to those of Guo,³⁵ who showed that *P.linteus*(PL) and *Ganoderma lucidum* (GL) suppressed the growth of Bel-7404 cells through S phase cell cycle arrest, mediated by the inhibition of Cyclin E/CDK2 activities.

Microfilament and microtubule were the main components of the cytoskeleton. The cytoskeleton played an important role in the process of mitosis³⁶ and M phase was the mitotic phase. To examine the mechanism of cell cycle arrest at G2/M phase, the changes in microfilament, microtubule, the nucleus and the process of mitosis in cells after exposure to endosulfan were observed. Results showed that the number of microfilaments and microtubules significantly reduced, the maldistribution phenomenon of microfilaments and microtubules obviously increased, and the nucleus pycnosis was more frequently observed with the increase of endosulfan concentration. Moreover, some cells in 24 μ g/mL endosulfan treated group failed to complete mitosis process normally and died finally, which was similar to those of William. They showed that treatment with the ILK Inhibitor QLT-0267 resulted in a significant G2/M arrest as well as aberrant cytokinesis and mitotic spindle disorganization.³⁷ Hence, we inferred that endosulfan might inhibit the process of mitosis by causing the damages of microfilament, microtubule and nuclear. Blocking cell cycle progression may result in proliferation inhibition. So the proliferation were assessed. Results showed that endosulfan inhibited the proliferation of GC-1spg cells. But the result of Tellez-Banuelos showed that low concentration of endosulfan

increased cellular proliferation in spleen cells,⁵ which was different with our results. This may be because the doses of endosulfan and cell lines used in the experiments were different. To investigate the possible mechanism of cell proliferation inhibition induced by endosulfan, the related signaling pathways of cell cycle were further studied. The mitogen-activated protein kinases (MAPKs) were serine/threonine kinases which played a vital role in controlling proliferation. Among them, the ERK family including ERK1 and ERK2 were proven to be implicated.³⁸ In proliferation, the PKC- α -RAF-1-MEK1/2-ERK1/2 pathway was involved.³⁹ So the expression of ERK1/2, *p*-ERK1/2, MEK1/2, *p*-MEK1/2 and RAF-1 were measured. Our results showed that endosulfan induced the down-regulation of RAF-1, MEK1/2, *p*-MEK1/2, ERK1/2 and *p*-ERK1/2 expression, which was similar to those of Levinthal.⁴⁰ The study of Levinthal using murine neuronal cells had shown that glutamate-induced oxidative stress specifically inhibited the phosphatase activity by the down-regulation of ERK1/2 expression (PP2A, MKPs). However, the previous study had shown that endosulfan could activate ERK1/2 via PKC-RAF-MEK1/2-dependent and PKC-MEK1/2-dependent pathways in human HaCaT cells.⁴¹ Our results suggested that endosulfan inhibited ERK1/2 via PKC- α -RAF-1-MEK1/2-dependent pathway in GC-1spg cells. So we deduced that different kinds of cells might have different responses to various concentration of endosulfan.

The previous findings indicated that Cyclins and Cyclin dependent kinase (CDK)

were downstream mediators of the growth-regulatory activity of Irf-1,⁴²⁻⁴⁴ and blocking ERK1/2 pathway inhibited Irf-1-mediated proliferation.⁴⁵ The results indicated that inhibition of ERK1/2 pathway might cause the down-regulation of Cyclins and CDK expression, which was the same with our results. Hence, the molecular mechanism may be that endosulfan could induce the cell cycle arrest and proliferation inhibition by inhibiting the protein expression of PKC- α -RAF-1-MEK1/2-ERK1/2 pathway because of DNA damage resulted from oxidative stress and down-regulating the protein expression of Cyclin E and CDK2; meanwhile, endosulfan could also lead to mitotic arrest through directly damaging the cytoskeleton and cell nucleus resulted from oxidative stress; which therefore induced cytotoxicity of GC-1spg cells.

In summary, endosulfan could cause the cytotoxicity of GC-1spg cells by the following two pathways (1) endosulfan could induce cell cycle arrest at S phase and proliferation inhibition by inhibiting the protein expression of cellular signaling pathway mediated by PKC- α ; (2) endosulfan could lead to cell cycle arrest at G2/M phase through directly damaging the microfilament, microtubule and the cell nucleus. The finding provides new evidence to explain the endosulfan-induced male reproductive toxicity and reveals new potential downstream pathway. It is important to understand the mechanism of reproductive toxicity from endosulfan and prevent from it. However, additional work is required to explore the precise mechanism responsible for endosulfan-induced male reproductive toxicity *in vivo*, such as

signaling pathway related to meiosis. Moreover, management should be more strict in additional risks of endosulfan exposure in certain subpopulations, for example, people who have the disease of reproductive system.

Acknowledgements

This research was supported by the National Natural Science Foundation of China (No. 31172086).

References

1. Becker L, Scheringer M, Schenker U, Hungerbuhler K. Assessment of the environmental persistence and long-range transport of endosulfan. *Environ Pollut.* 2011; 159:1737-43.
2. Desalegn B, Takasuga T, Harada KH, Hitomi T, Fujii Y, Yang HR, et al. Historical trends in human dietary intakes of endosulfan and toxaphene in China, Korea and Japan. *Chemosphere.* 2011; 83: 1398-405.
3. Abdul Majeed S, Nambi KS, Taju G, Sarath Babu V, Farook MA, Sahul Hameed AS. Development and characterization of a new gill cell line from air breathing fish *Channa striatus* (Bloch 1793) and its application in toxicology: direct comparison to the acute fish toxicity. *Chemosphere.* 2014; 96:89-98.
4. EJF. End of the Road for Endosulfan: A Call for Action Against a Dangerous Pesticide. Environmental Justice Foundation. 2002.
5. Tellez Banuelos MC, Ortiz Lazareno PC, Santerre A, Casas Solis J, Bravo Cuellar A, Zaitseva G. Effects of low concentration of endosulfan on proliferation, ERK1/2 pathway, apoptosis and senescence in Nile tilapia (*Oreochromis niloticus*) splenocytes. *Fish Shellfish Immun.* 2011; 31:1291-1296.
6. Ernst WR, Jonah P, Doe K, Julien G, Hennigar P. Toxicity to aquatic organisms of off-target deposition of endosulfan applied by aircraft. *Environ Toxicol Chem.* 1991; 10:103-114.
7. Singh ND, Sharma AK, Dwivedi P, Patil RD, Kumar M. Citrinin and endosulfan induced teratogenic effects in Wistar rats. *Journal of applied toxicology : JAT.* 2007; 27:143-51.
8. Harner T, Pozo K, Gouin T, Macdonald AM, Hung H, Caine J, et al. Global pilot study for persistent organic pollutants (POPs) using PUF disk passive air samplers. *Environ Pollut.* 2006; 144:445-452.
9. Chaudhuri K, Selvaraj S, Pal AK. Studies on the genotoxicity of endosulfan in bacterial systems. *Mutat Res-Gen Tox En.* 1999; 439:63-67.
10. Paul V, Balasubramaniam E, Jayakumar AR, Kazi MA. Sex-Related Difference In the Neurobehavioral And Hepatic-Effects Following Chronic Endosulfan Treatment In Rats. *Eur J Pharm-Environ.* 1995; 293:355-360.
11. Jamil K, Shaik AP, Mahboob M, Krishna D. Effect of organophosphorus and organochlorine

- pesticides (monochrotophos, chlorpyriphos, dimethoate, and endosulfan) on human lymphocytes in-vitro. *Drug Chem Toxicol.* 2004; 27:133-144.
12. Aggarwal M, Narahariseti SB, Dandapat S, Degen GH, Malik JK. Perturbations in immune responses induced by concurrent subchronic exposure to arsenic and endosulfan. *Toxicology.* 2008; 251:51-60.
 13. Choudhary N, Joshi SC. Reproductive toxicity of endosulfan in male albino rats. *Bulletin of environmental contamination and toxicology.* 2003; 70:285-289.
 14. Han Z, Jiao S, Kong D, Shan Z, Zhang X. Effects of beta-endosulfan on the growth and reproduction of zebrafish (*Danio rerio*). *Environmental toxicology and chemistry / SETAC.* 2011; 30: 2525-31.
 15. Song MO, Lee CH, Yang HO, Freedman JH. Endosulfan upregulates AP-1 binding and ARE-mediated transcription via ERK1/2 and p38 activation in HepG2 cells. *Toxicology.* 2012; 292:23-32.
 16. Gao X, Wang Q, Wang J, Wang C, Lu L, Gao R, et al. Expression of calmodulin in germ cells is associated with fenvalerate-induced male reproductive toxicity. *Archives of toxicology.* 2012; 86: 1443-51.
 17. Aly HA, Khafagy RM. Taurine reverses endosulfan-induced oxidative stress and apoptosis in adult rat testis. *Food and chemical toxicology : an international journal published for the British Industrial Biological Research Association.* 2014; 64:1-9.
 18. Choudhary N, Joshi SC. Reproductive toxicity of endosulfan in male albino rats. *Bulletin of environmental contamination and toxicology.* 2003; 70:285-9.
 19. Takhshid MA, Tavasuli AR, Heidary Y, Keshavarz M, Kargar H. Protective effect of vitamins e and C on endosulfan-induced reproductive toxicity in male rats. *Iranian journal of medical sciences.* 2012; 37: 173-80.
 20. Wang N, Qian HY, Zhou XQ, Li YB, Sun ZW. Mitochondrial energy metabolism dysfunction involved in reproductive toxicity of mice caused by endosulfan and protective effects of vitamin E. *Ecotoxicology and environmental safety.* 2012; 82:96-103.
 21. Duan J, Yu Y, Li Y, Yu Y, Li Y, Zhou X, et al. Toxic effect of silica nanoparticles on endothelial cells through DNA damage response via Chk1-dependent G2/M checkpoint. *PloS one.* 2013; 8:e62087.
 22. Nath KA, Croatt AJ, Likely S, Behrens TW, Warden D. Renal oxidant injury and oxidant response induced by mercury. *Kidney international.* 1996; 50:1032-43.
 23. Kannan RR, Iniyan AM, Prakash VS. Isolation of a small molecule with anti-MRSA activity from a mangrove symbiont *Streptomyces* sp. PVRK-1 and its biomedical studies in Zebrafish embryos. *Asian Pacific journal of tropical biomedicine.* 2011; 1:341-7.
 24. Guo R, Li W, Liu B, Li S, Zhang B, Xu Y. Resveratrol protects vascular smooth muscle cells against high glucose-induced oxidative stress and cell proliferation in vitro. *Medical science monitor basic research.* 2014; 20:82-92.
 25. Meira LB, Bugni JM, Green SL, Lee CW, Pang B, Borenshtein D, et al. DNA damage induced by chronic inflammation contributes to colon carcinogenesis in mice. *The Journal of clinical investigation.* 2008; 118:2516-25.
 26. Tao Y, Pan L, Zhang H, Tian S. Assessment of the toxicity of organochlorine pesticide endosulfan in clams *Ruditapes philippinarum*. *Ecotoxicology and environmental safety.* 2013; 93:22-30.
 27. Lukin DJ, Carvajal LA, Liu WJ, Resnick Silverman L, Manfredi JJ. p53 Promotes Cell Survival Due to the Reversibility of its Cell Cycle Checkpoints. *Molecular cancer research : MCR.* 2014.
 28. Abraham RT. Cell cycle checkpoint signaling through the ATM and ATR kinases. *Genes & development.* 2001; 15:2177-2196.

29. Grana X, Reddy EP. Cell cycle control in mammalian cells: role of cyclins, cyclin dependent kinases (CDKs), growth suppressor genes and cyclin-dependent kinase inhibitors (CKIs). *Oncogene*. 1995; 11: 211-9.
30. Black AR, Black JD. Protein kinase C signaling and cell cycle regulation. *Frontiers in immunology*. 2012; 3:423.
31. Livneh E, Fishman DD. Linking protein kinase C to cell-cycle control. *European journal of biochemistry / FEBS*. 1997; 248:1-9.
32. Newton AC. Lipid activation of protein kinases. *Journal of lipid research*. 2009; 50 Suppl:S266-71.
33. Haughian JM, Reno EM, Thorne AM, Bradford AP. Protein kinase C alpha-dependent signaling mediates endometrial cancer cell growth and tumorigenesis. *International journal of cancer. Journal international du cancer*. 2009; 125:2556-64.
34. Detjen KM, Brembeck FH, Welzel M, Kaiser A, Haller H, Wiedenmann B, et al. Activation of protein kinase C alpha inhibits growth of pancreatic cancer cells via p21(cip)-mediated G(1) arrest. *Journal of cell science*. 2000; 113 (Pt 17): 3025-35.
35. Guo J, Zhu T, Collins L, Xiao ZX, Kim SH, Chen CY. Modulation of lung cancer growth arrest and apoptosis by *Phellinus linteus*. *Molecular carcinogenesis*. 2007; 46:144-54.
36. Ritchey L, Chakrabarti R. Aurora A kinase modulates actin cytoskeleton through phosphorylation of Cofilin: Implication in the mitotic process. *Biochimica et biophysica acta*. 2014; 1843:2719-2729.
37. Sikkema WK, Strikwerda A, Sharma M, Assi K, Salh B, Cox ME, et al. Regulation of mitotic cytoskeleton dynamics and cytokinesis by integrin-linked kinase in retinoblastoma cells. *PloS one*. 2014; 9:e98838.
38. Chang LF, Karin M. Mammalian MAP kinase signalling cascades. *Nature*. 2001; 410:37-40.
39. Tellez Banuelos MC, Ortiz Lazareno PC, Santerre A, Casas Solis J, Bravo Cuellar A, Zaitseva G. Effects of low concentration of endosulfan on proliferation, ERK1/2 pathway, apoptosis and senescence in Nile tilapia (*Oreochromis niloticus*) splenocytes. *Fish Shellfish Immunol*. 2011; 31:1291-6.
40. Levinthal DJ, Defranco DB. Reversible oxidation of ERK-directed protein phosphatases drives oxidative toxicity in neurons. *The Journal of biological chemistry*. 2005; 280:5875-83.
41. Lédirac N, Antherieu S, d'Uby AD, Caron JC, Rahmani R. Effects of organochlorine insecticides on MAP kinase pathways in human HaCaT keratinocytes: key role of reactive oxygen species. *Toxicological sciences : an official journal of the Society of Toxicology*. 2005; 86:444-52.
42. Bowie ML, Ibarra C, Seewalt VL. IRF-1 promotes apoptosis in p53-damaged basal-type human mammary epithelial cells: a model for early basal-type mammary carcinogenesis. *Advances in experimental medicine and biology*. 2008; 617:367-74.
43. Xie RL, Gupta S, Miele A, Shiffman D, Stein JL, Stein GS, et al. The tumor suppressor interferon regulatory factor 1 interferes with SP1 activation to repress the human CDK2 promoter. *The Journal of biological chemistry*. 2003; 278:26589-96.
44. Chen FF, Jiang G, Xu KR, Zheng JN. Function and mechanism by which interferon regulatory factor-1 inhibits oncogenesis (Review). *Oncol Lett*. 2013; 5:417-423.
45. Zhang X, Liu L, Chen C, Chi YL, Yang XQ, Xu Y, et al. Interferon regulatory factor-1 together with reactive oxygen species promotes the acceleration of cell cycle progression by up-regulating the cyclin E and CDK2 genes during high glucose-induced proliferation of vascular smooth muscle cells. *Cardiovascular diabetology*. 2013; 12.

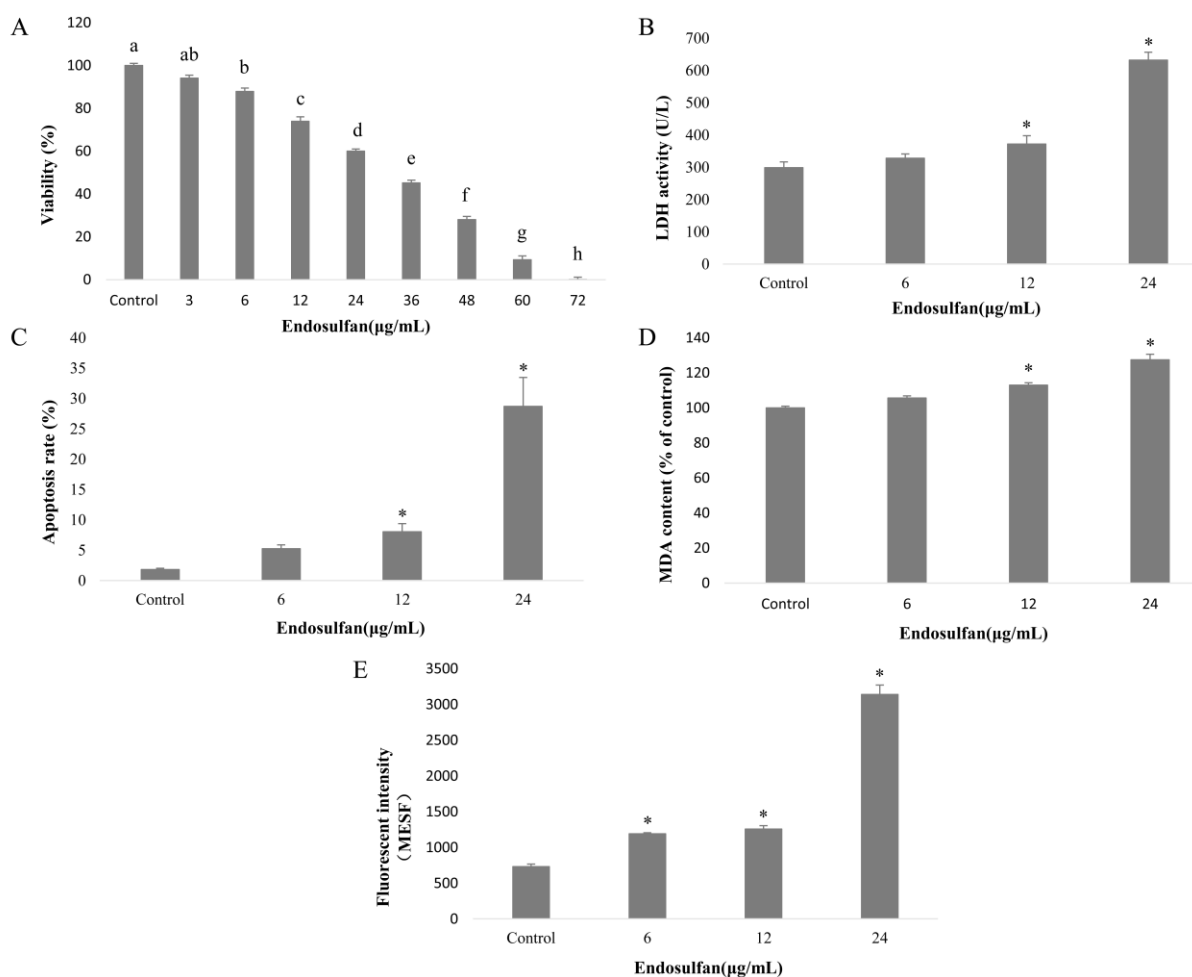


Figure 1.

Cytotoxicity and Oxidative Damage of GC-1spg Cells Induced by Endosulfan

(Means \pm S.E.) . (A) Cell viability of GC-1spg cells treated with various concentrations of endosulfan for 24 h was measured by MTT assay. Values with entirely different superscripts were significantly different ($P < 0.05$) (B) LDH leakage of GC-1spg cells exposed to various concentrations of endosulfan for 24 h. (C) The sum of early apoptosis rate and late apoptosis rate was finally calculated as the apoptosis rate. (D) The MDA level of GC-1spg cells exposed to various concentrations of endosulfan for 24 h. (E) The ROS level of GC-1spg cells exposed to various concentrations of endosulfan for 24 h.

* indicated significant difference compared to control group ($P < 0.05$)

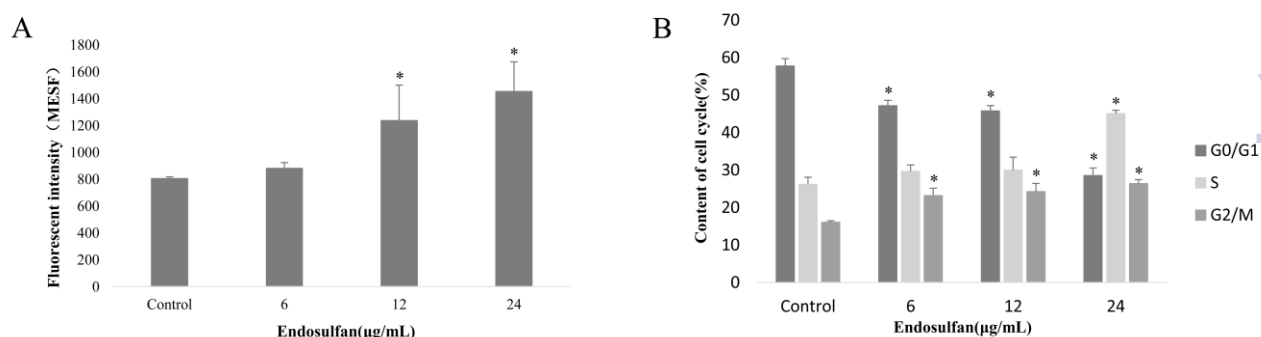


Figure 2.

Proliferation Inhibition and Cell Cycle Arrest of GC-1spg Cells Induced by

Endosulfan (Means±S.E.) . (A) After exposure to various concentrations of endosulfan for 24 h, the proliferation of GC-1spg cells were determined using flow cytometry . The increase of average fluorescence intensity in cells indicated cellular proliferation were inhibited. (B) After exposure to different concentrations of endosulfan for 24h, the cell cycle distribution of GC-1spg cells was measured by flow cytometry.

* indicated significant difference compared to control group ($P < 0.05$)

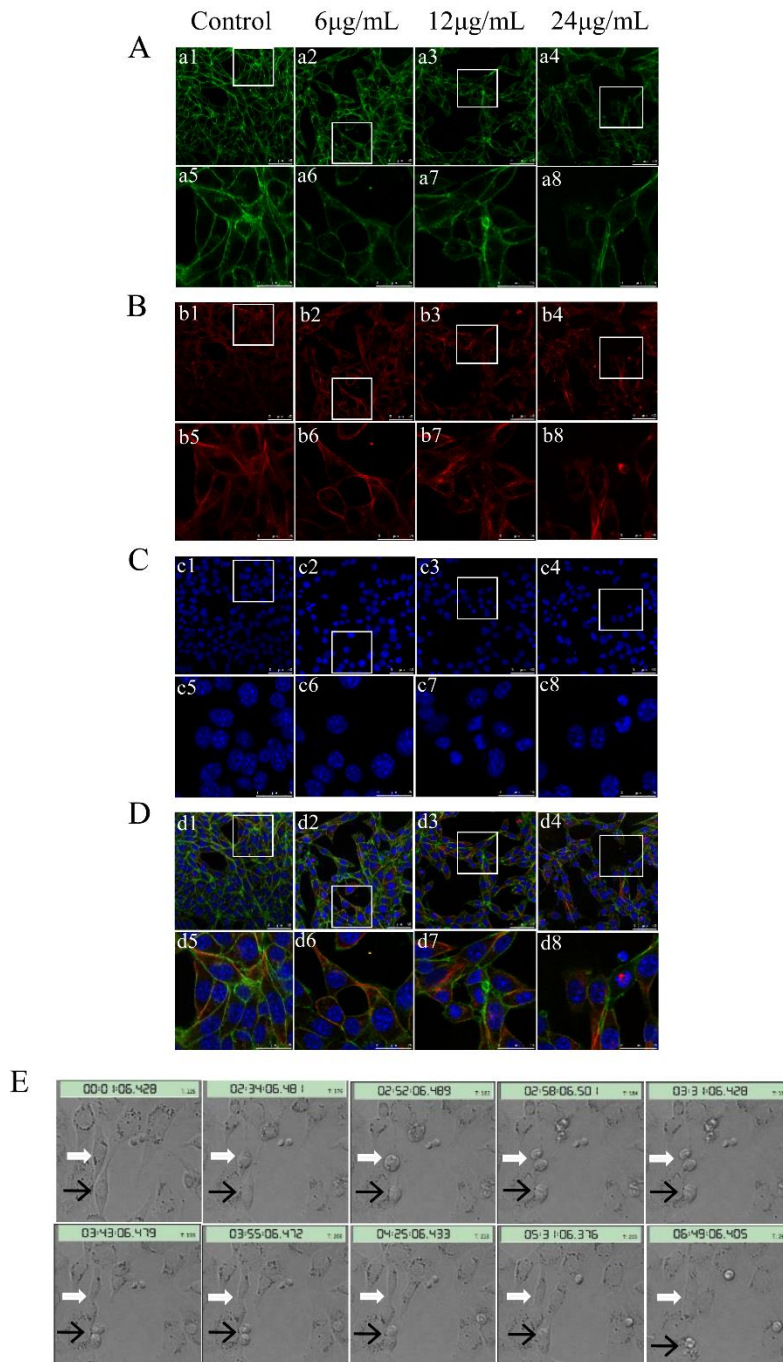


Figure 3.

Changes of the Microfilament, Microtubule, Cell Nucleus and the Mitosis

Process Induced by Endosulfan. After exposure to various concentrations of endosulfan for 24 h, the changes in microfilament, microtubule, cell nucleus and the mitosis process were visualized using a laser confocal microscope. (A)The

microfilament was stained with Actin-Tracker Green. The images from a5 to a8 were the images magnified double from a1 to a4, respectively. (B) The microtubule was stained with Tubulin-Tracker Red. The images from b5 to b8 were the images magnified double from b1 to b4, respectively. (C) The cell nucleus was stained with Hoechst 33258 solution. The images from c5 to c8 were the images magnified double from c1 to c4, respectively. (D) The images were the composite images of microfilament, microtubule and cell nucleus. The images from d5 to d8 were the images magnified double from d1 to d4, respectively. (E) The cells were incubated with 24 $\mu\text{g}/\text{mL}$ endosulfan and observed for 24h by a real-time inverted phase contrast microscope. Six fields were selected randomly and taken pictures every 10 minutes. In the images, the white arrow pointed to the normal mitosis process and the black arrow pointed to the abnormal mitosis process.

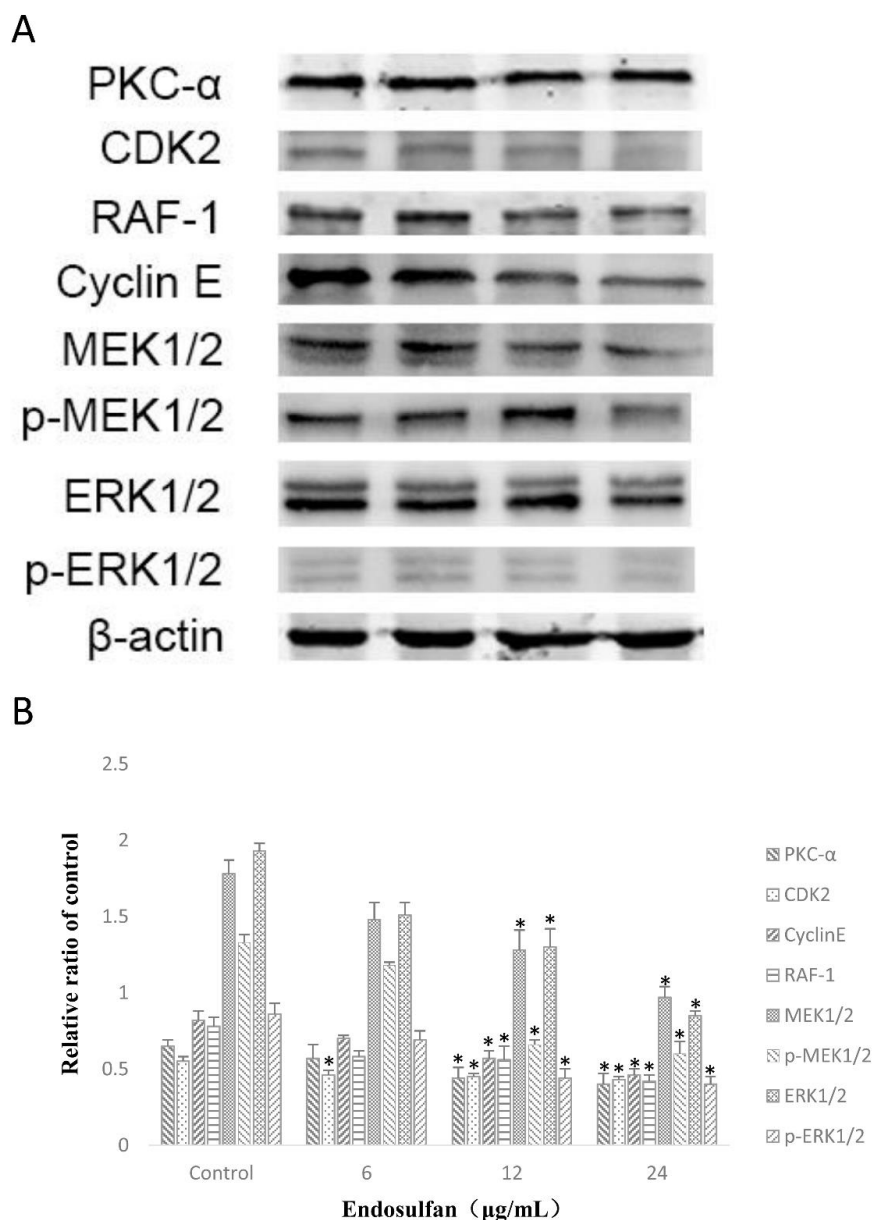


Figure 4.

Effect of Endosulfan on the Cellular Signaling Pathway Mediated by PKC- α

(Means \pm S.E.). (A) Effect of endosulfan on the protein expression of PKC- α , CDK2, Cyclin E, RAF-1, MEK1/2, *p*-MEK1/2, ERK1/2 and *p*-ERK1/2. β -actin was used as an internal control to monitor for equal loading. (B) Relative densitometric analysis of the proteins bands was carried out and presented.

* indicated significant difference compared to control group ($P < 0.05$)

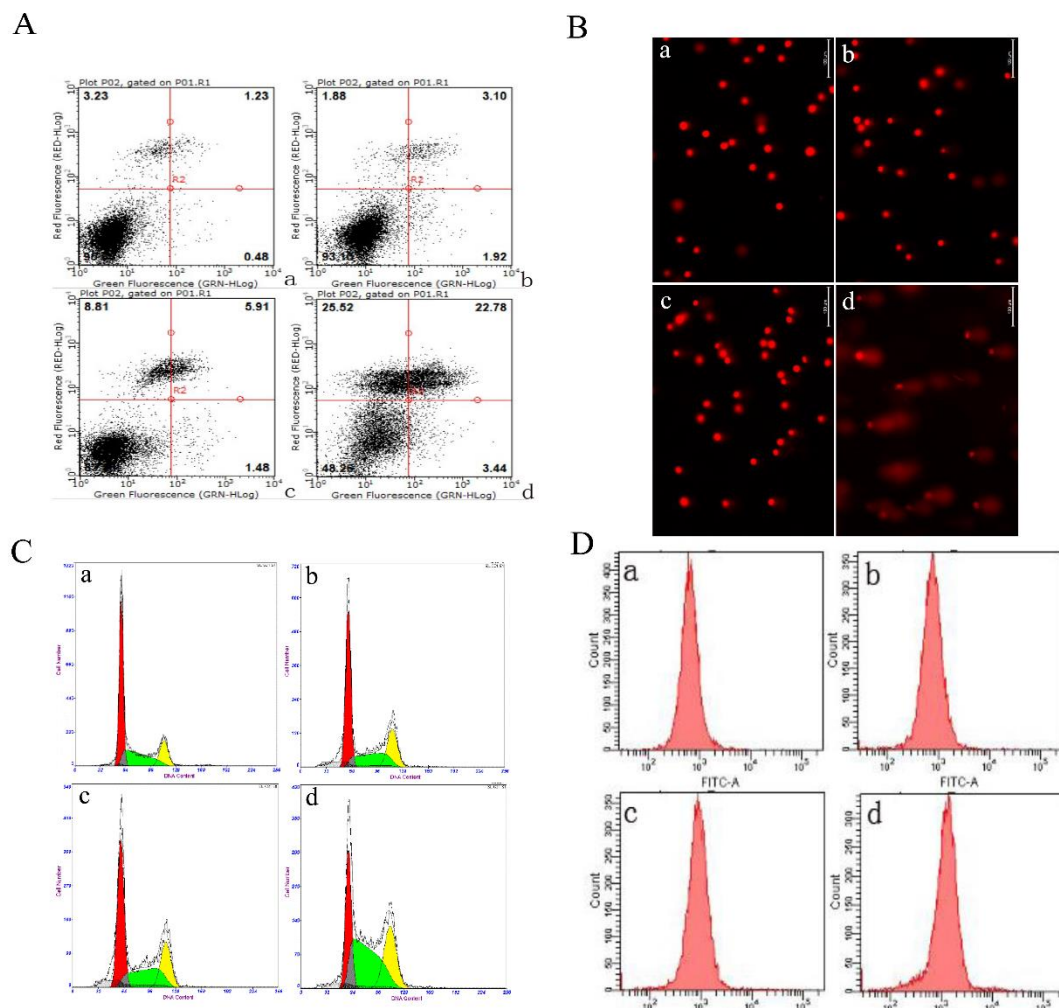


Figure 5.

The Images of Apoptosis, DNA Damage, Cell Cycle Arrest and Proliferation

Inhibition of GC-1spg Cells after Exposure to Endosulfan for 24h (A) a-d:

Control group(a), 6 $\mu\text{g/mL}$ endosulfan group(b), 12 $\mu\text{g/mL}$ endosulfan group (c),

24 $\mu\text{g/mL}$ endosulfan group (d). Apoptotic populations of cells double stained with PI-

and FITC-labeled Annexin V were described by flow cytometry. (B) a-d: Control group

200 \times (a), 6 $\mu\text{g/mL}$ endosulfan group 200 \times (b), 12 $\mu\text{g/mL}$ endosulfan group 200 \times (c),

24 μ g/mL endosulfan group 200 \times (d). DNA damage of GC-1spg cells treated with various concentrations of endosulfan for 24 h was measured by Comet assay. More severe DNA damage was reflected by larger area of the comet tail. (C) a-d: Control group (a), 6 μ g/mL endosulfan group (b), 12 μ g/mL endosulfan group (c), 24 μ g/mL endosulfan group (d). The red area, green area and yellow area represented the G0/G1, S and G2/M phase, respectively. (D) a-d: Control group(a), 6 μ g/mL endosulfan group(b), 12 μ g/mL endosulfan group (c), 24 μ g/mL endosulfan group (d). The abscissa value of peak was the average fluorescence intensity of cells.

Table 1.

Cytotoxicity of GC-1spg Cells Induced by Endosulfan

| Concentration (μ g/mL) | Cell viability (% of control) |
|--------------------------------|----------------------------------|
| 0 | 100 |
| 4.397 | 90 |
| 11.505 | 80 |
| 18.613 | 70 |
| 25.721 | 60 |
| 32.829 | 50 |
| 39.937 | 40 |
| 47.045 | 30 |
| 54.153 | 20 |
| 61.261 | 10 |

Table 2.**DNA Damage of GC-1spg Cells Induced by Endosulfan**

| Concentration ($\mu\text{g/mL}$) | Tail length | Tail DNA (%) | Tail movement | Olive tail movement |
|---------------------------------------|-------------------|-------------------|-------------------|------------------------|
| 0 | 18.30 \pm 0.90 | 8.20 \pm 0.47 | 1.59 \pm 0.22 | 2.19 \pm 0.23 |
| 6 | 22.47 \pm 0.81 | 9.24 \pm 0.46 | 2.52 \pm 0.20 | 2.64 \pm 0.19 |
| 12 | 22.53 \pm 1.18 | 9.25 \pm 0.50 | 3.56 \pm 0.40 | 3.34 \pm 0.29 |
| 24 | 69.65 \pm 2.04* | 54.64 \pm 0.81* | 58.85 \pm 2.04* | 39.94 \pm 1.07* |

* indicated significant difference compared to control group ($P < 0.05$)